One-step hydroxylation of benzene to phenol. II. Gas phase N_2O oxidation over Mo / Fe / borosilicate molecular sieve

Jin S. Yoo [1], A.R. Sohail, S. Scott Grimmer and Chin Choi-Feng

Amoco Chemical Company, Amoco Research Center, PO Box 3011,
Naperville, IL 60566, USA

Received 12 April 1994; accepted 10 August 1994

The Fe/Mo/partially deboronated borosilicate molecular sieve catalyst prepared by the chemical vapor deposition (CVD) method was active for the selective formation of phenol by gas-phase N_2O oxidation of benzene. The impregnated counterpart exhibited lower activity than the CVD catalyst. The borosilicate molecular sieve itself also was active. Two mechanistic paths are postulated based on reactive oxygen species such as O^-, which can be generated via interaction of N_2O with the iron sites in the CVD-borosilicate molecular sieve catalyst, or OH^+, which can be generated by Brønsted sites on the borosilicate molecular sieve itself.

Keywords: gas phase oxidation; N_2O; benzene; phenol; CVD Fe/Mo/borosilicate; impregnated catalyst; borosilicate molecular sieve

1. Introduction

Phenol has been synthesized by an oxidation of cumene through multistep procedures [1], while direct hydroxylation of benzene has long been sought as a desirable process. It has been demonstrated that phenol can readily be synthesized from benzene with air in aqueous solutions containing Cu^+ ions with and without heterogeneous catalysts such as Pd/SiO_2 [2,3].

We found that the silica coformed $Fe/Mo/SiO_2$ catalyst was effective for direct hydroxylation of benzene to phenol by the gas-phase nitric acid oxidation in a previous study [4]. In an effort to circumvent drawbacks inherent in the gas-phase nitric acid oxidation processes, nitrous oxide, N_2O, was selected as an alternate oxidant.

In recent years, nitrous oxide has attracted considerable attention as a unique oxidant, especially in a search for ways to activate methane and other lower paraffins over various catalysts including zeolite [5–9].

---

[1] To whom correspondence should be addressed.

Nitrous oxide can be an attractive active oxygen source for a variety of oxidation reactions because it is thermodynamically unstable,

$$2N_2O \rightarrow 2N_2 + O_2 \qquad \Delta G = -25 \text{ kcal/mol},$$

and kinetically inert in the absence of an activating center. Since a significant quantity of inexpensive N_2O is readily available as a byproduct of adipic acid manufacturing processes, applications utilizing N_2O become commercially quite attractive.

Recently, the direct hydroxylation of benzene to phenol using nitrous oxide as an oxidant was studied over a range of zeolitic catalysts [10–12]. It has been found that ZSM-5 is an excellent catalyst for the reaction, achieving up to 99% selectivity at low conversions, and the phenol yields attained from these runs are in the range of 15.44–27.2%. Zeolites having the EU-1 type structure showed low activities and selectivities, while amorphous acidic silica–alumina catalysts were inactive. The same reaction was also studied over H-ZSM-5 doped with iron [13–15]. The activity of Fe on the zeolite was found to be higher by several orders of magnitude than its activity on Fe_2O_3. A reactive surface oxygen species generated by N_2O on specific active sites consisting of Fe atoms has been postulated to be responsible for the catalytic properties observed. In these reactions, nitrous oxide decomposition is believed to be the rate-limiting step in the catalytic cycle [16,17].

The same hydroxylation of benzene was also studied by others. Iwamoto et al. produced phenol with a selectivity (71%) by the reaction of benzene in N_2O at 550–600°C over supported oxides of V, Mo, or W [18–21]. The selective phenol synthesis was further pursued by another group, and it was reported that benzene could be oxidized over H-ZSM-5 molecular sieve using N_2O at lower temperatures, 300–400°C, with a good efficiency [27–29]. These novel findings prompt us to look into the N_2O oxidation of benzene to phenol over CVD and impregnated Fe/Mo/partially deboronated borosilicate molecular sieve HAMS-1B-3 (DBH) catalyst, silica coformed Fe/Mo/SiO_2, and borosilicate molecular sieve itself without metal deposition.

2. Experimental

2.1. PREPARATION OF CATALYSTS

Catalyst A, CVD Fe/Mo/DBH, the CVD Fe/Mo/partially deboronated borosilicate molecular sieve (DBH) catalyst was prepared from $FeCl_3$ and MoO_2Cl_2 with the borosilicate molecular sieve (HAMS-1B-3) containing 1.21 wt% B, 440 ppm Al, 256 ppm Fe and 157 ppm Pb as impurities, and having a surface area of 373 m^2/g, in two steps by the chemical vapor deposition technique according to the procedure described elsewhere [30]. The CVD Fe/DBH was prepared by depositing $FeCl_3$ vapor on the borosilicate molecular sieve in the first step. The resulting

Fe/DBH containing 41% Si, 0.15% B, and 2.2% Fe was subjected to the chemical vapor deposition of MoO_2Cl_2 in the subsequent step to prepare CVD Fe/Mo/DBH. The calcined final CVD Fe/Mo/DBH catalyst contained 4.6% Mo, 1.41% Fe, and an atomic ratio of Mo/Fe = 1.92, and its surface area was 288 m^2/g.

Catalyst B, the impregnated Fe/Mo/DBH catalyst, was prepared from aqueous solutions of $Fe(NO_3)_3$, ammonium paramolybdate and borosilicate molecular sieve by the standard incipient wetness method.

Catalyst C, silica coformed $Fe/Mo/SiO_2$ catalyst, was prepared from $Fe(NO_3)_3$, ammonium paramolybdate and Nalco silica gel 1034A according to the procedure described elsewhere [4].

2.2. N_2O OXIDATION OF BENZENE

The N_2O oxidation of benzene was studied over catalysts A and B in the gas phase, and the results were compared with those obtained with catalysts C and D under identical conditions. The 20–40 mesh sizes of these calcined catalysts were loaded in a quartz reactor (o.d. 1 inch), and the N_2O oxidation of benzene was carried out by feeding benzene and N_2O separately into the catalyst bed under the following conditions:

catalyst load: 16–18 ml (4.27–14.0 g)
LHSV of benzene: 0.1/h
molar ratio of N_2O : benzene: 6–9 : 1
temperatures: 230–425°C
carrier gas: none

The products were identified by GC/mass spectrometry, and quantitatively analyzed by the method described in a previous paper [4].

2.3. CHARACTERIZATION OF CATALYSTS

The surface properties of catalysts A, B, C, and D, borosilicate molecular sieve itself (HAMS-1B-3) were determined, and the results are summarized in table 1.

Catalysts A and D were subjected to an ammonia temperature programmed desorption (TPD) study together with CVD Fe/DBH intermediate material deposited with the $FeCl_3$ vapor alone before the MoO_2Cl_2 vapor was deposited in the subsequent step to complete the preparation of catalyst A, CVD Fe/Mo/DBH. The results are shown in table 2, and plotted in fig. 1. Catalyst D showed a weak acid site at 172°C. An additional stronger acidic site appeared at 319°C and a weak site at 178°C on CVD Fe/DBH. This stronger acid site disappeared to yield a relatively weak acid site at 195°C when the MoO_2Cl_2 vapor was deposited on CVD Fe/DBH in the subsequent step.

Raman spectra of catalysts A and B are compared in fig. 2. The Raman spectra of catalysts A and B were virtually identical except that an additional α-Fe_2O_3

Table 1
Physical properties of Mo/M/DBH

Catalyst	Mo (wt%)	Fe (wt%)	Mo/Fe	BET surface area (m^2/g)	Micropore vol. (cm^3/g)	Micropore radius[a] (Å)
A, CVD Fe/Mo/DBH	4.60	1.40	1.9	288	0.111	
[spent]	4.15	1.43	1.6	296	0.088	25
B, Fe/Mo/DBH (impregnated)	4.50	1.50	1.75	313	0.118	
[spent]				315	0.102	19
C, Fe/Mo/SiO_2 (coformed)	2.58	0.93	1.61	110	0.252	31
[spent]	2.58	0.93	1.46	95	0.227	32
D, HAMS-1B-3[b]	B: 1.36					
	Cl: 0.27			294	0.133	55
[spent]				301	0.130	52

[a] Measured by the adsorption method.

[b] Prepared in ethylenediamine, and HAMS-1B-1 was prepared in a caustic medium.

phase appeared in catalyst B besides the $Fe_2(MoO_4)_3$ and MoO_3 phases identified in catalyst A.

The transmission electron micrographs (TEM) of catalysts A and B are shown in fig. 3. The TEM revealed that in catalyst A, Fe and Mo are finely and uniformly deposited into partially deboronated borosilicate (DBH) primarily along the micropore channels. Thus cylindrical domains of Mo and Fe were observed in the CVD material. After calcination, most of these cylindrical domains have changed into nearly spherical domains via diffusion processes. However, nearly all Mo and Fe still reside inside the DBH sieve, as shown in fig. 3a. The compositions of the Mo/Fe rich phases were analyzed by energy dispersive X-ray spectrometry

Table 2
Ammonia temperature programmed desorption (TPD)

Catalyst	Pretreatment (°C)	Peak (°C)	Peak ($mm\ H^+/g$)	% Fe or B calc.	% Fe or B ICP	Surface area (m^2/g)
D, HAM-1B-3	600	172	0.69	0.75(B)	1.06(B)	330–353
CVD Fe/DBH	550	178	0.79	4.4(Fe)		329
		319	0.20	1.1(Fe)		
				5.5(Fe)	2.20(Fe)	
A, CVD Fe/Mo/DBH	550	195	0.40	2.46(Fe)	2.20(Fe)	288

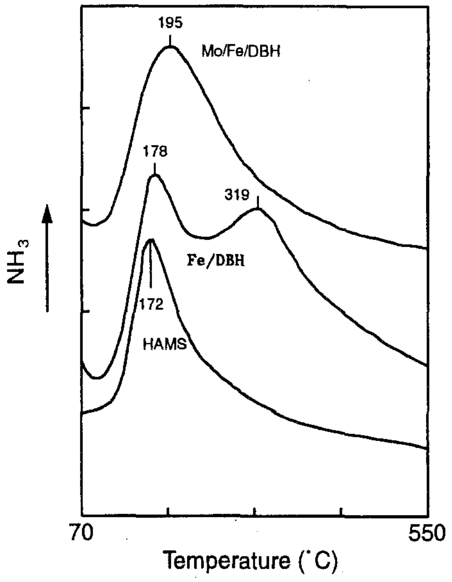

Fig. 1. Ammonia temperature programmed desorption (TPD).

(EDXS), which indicated that the Mo/Fe domains are predominantly ferric molybdate, $Fe_2(MoO_4)_3$.

On the other hand, larger aggregated particles were seen on mainly the exterior surface of the MFI structure in catalyst B, the impregnated counterpart. These results from the characterization study clearly bring out a unique structure resulting from the chemical vapor deposition preparation.

3. Results and discussion

The gas-phase N_2O oxidation of benzene was carried out over catalysts A, B and C in a quartz reactor by varying the temperatures. The representative results at different temperatures are compared in table 3. Among these three catalysts, catalyst A started to show the catalytic activity at 250°C. At 410°C, 17% of benzene was converted to phenol with a 97% selectivity. Over catalyst B, the conversion of benzene and the selectivity to phenol were 9% and almost 100% at 385–425°C, respectively. A very limited activity was seen with catalyst C.

With catalysts A and B, the phenol yields were tracked as a function of hours on stream by continually analyzing the samples collected in the designated time period at the designated temperatures, and plotted in fig. 4. With catalyst A, the reaction temperature was raised from 230 to 410°C in a 15 h period, and the reaction was continued at 410°C for another 15 h. With catalyst B, the initial reaction temperature, 330°C, was raised to 435°C in a 26 h period, and the run was kept on stream at 385–424°C for an additional 14 h. These results in fig. 4 also confirm an

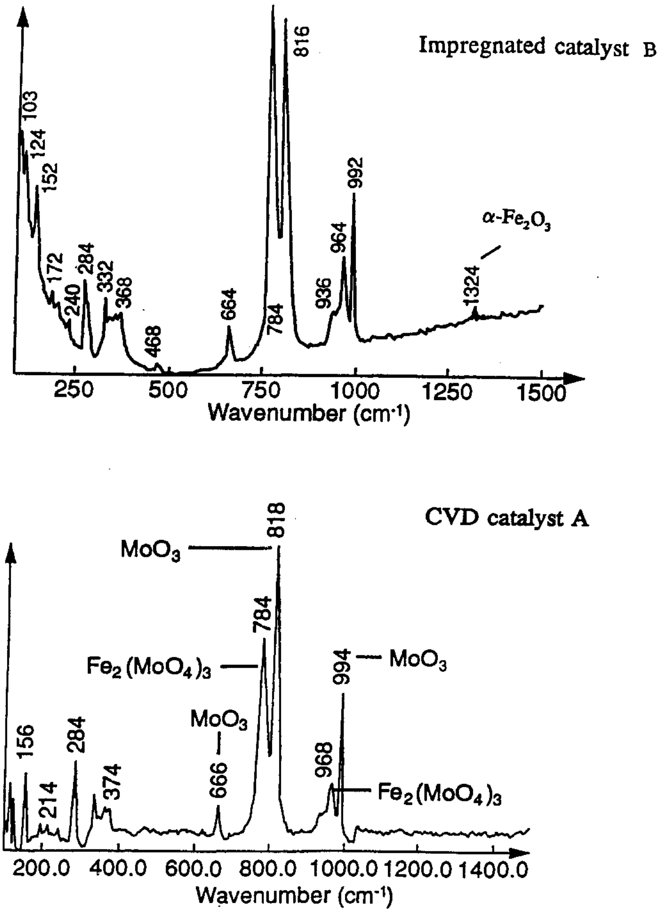

Fig. 2. Raman spectra of CVD and impregnated Fe/Mo/DBH.

earlier conclusion that catalyst A is more active than its impregnated counterpart, catalyst B, under similar reaction conditions, and that the phenol yield remains fairly constant at approximately 24 and 12% over catalyst A and B, respectively. Catalyst C, the silica coformed counterpart, shows very limited activity under similar conditions. In other words, the catalytic activity for the N_2O oxidation of benzene is in the order of: CVD Fe/Mo/DBH > impregnated Fe/Mo/DBH > coformed Fe/Mo/SiO_2. It appears that the supporting matrix and the catalyst preparation method play a key role for the gas-phase oxidation of benzene with N_2O, and that, as shown in the TEM in fig. 3, the uniformly dispersed fine ferric molybdate particles deposited along the main channel of the MFI structure are more effective than the large aggregated particles seen on the impregnated counterpart.

Catalyst A resulting from the above run was further subjected to other gas-phase oxidations with O_2, NO_2 and nitric acid intermittently over a prolonged period (approximately 150 h on stream), and the catalytic activity was maintained

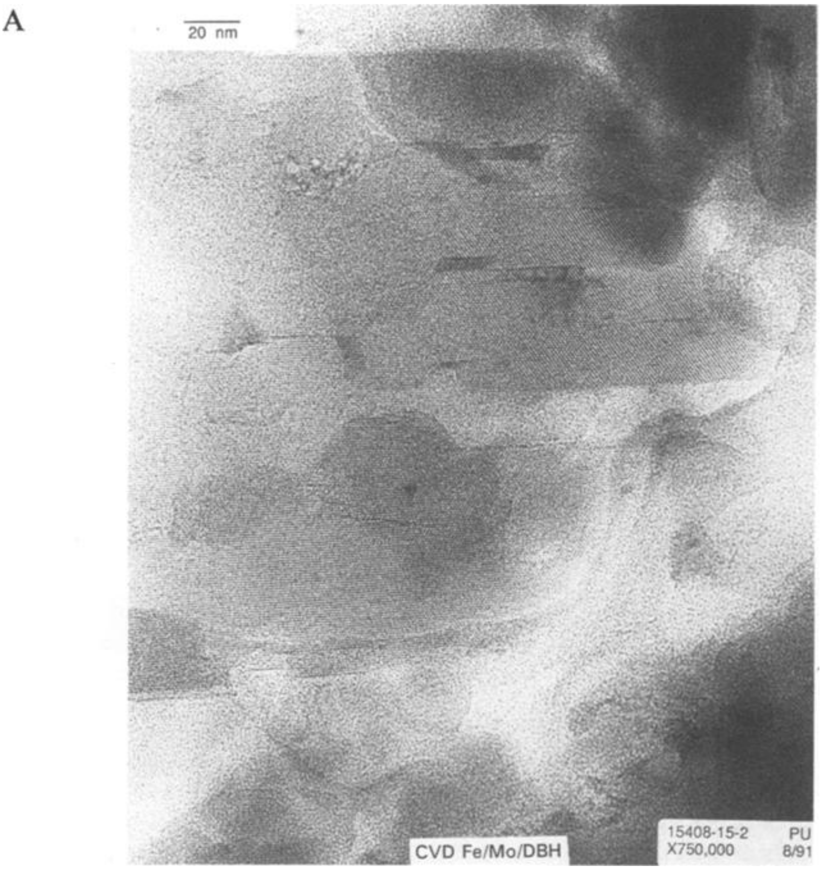

Fig. 3. TEM of catalysts A (CVD) and B (impregnated).

without showing any noticeable sign of deactivation. Metal levels found in the spent catalyst resulting from these runs seem to approach the stoichiometric composition of ferric molybdate, $Fe_2(MoO_4)_3$, as shown in table 1. The Raman spectrum of the spent catalyst indicates that MoO_3 is selectively sublimated off the catalyst matrix, but ferric molybdate remains unchanged [30].

Catalysts A and B failed to show any catalytic activity for the hydroxylation of benzene to phenol in runs with O_2 in place of N_2O, but they were active for the formation of phenol and nitrobenzene in NO_2 and nitric acid at 300°C. As stated earlier, we have already reported a study on gas-phase nitric acid oxidation of benzene to phenol [4].

Based on these results, one can conclude that the N_2O molecule probably interacts with iron sites in the ferric molybdate phase on the DBH matrix to generate a reactive surface oxygen species that cannot be produced with diatomic oxygen, O_2. Recently, individual properties of oxygen species such as $O^-, O_2^-, O^{2-}, O_3^-$ and OH^- on metal oxide catalysts have attracted considerable attention in defining the functions of these species for catalytic oxidation processes [18–26]. It has been con-

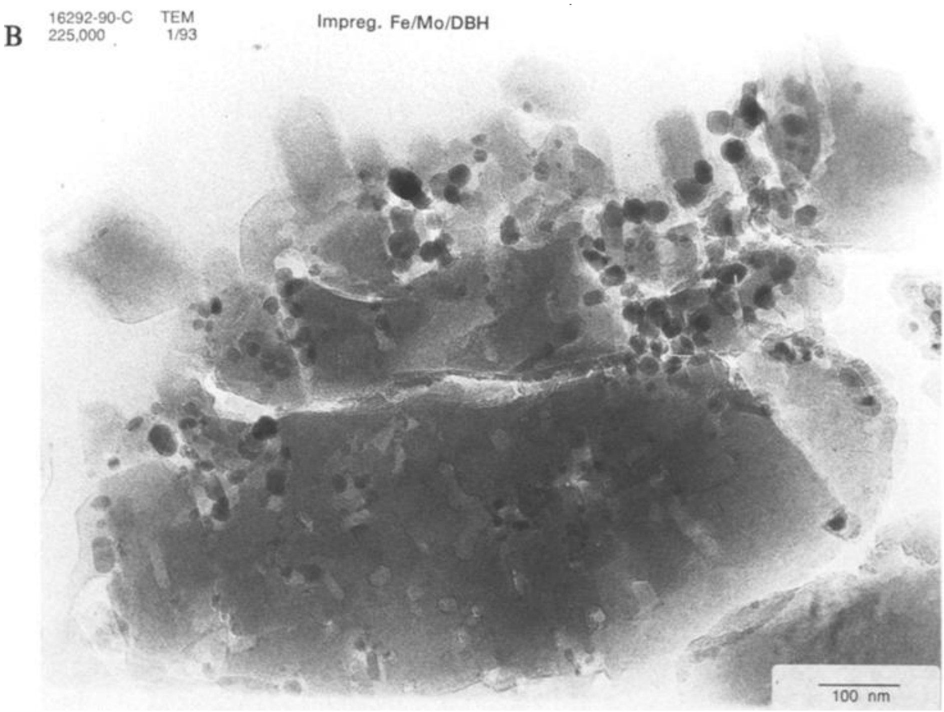

Fig. 3. (Continued.)

firmed by ESR, XPS, and TPD etc. that O^- can be generated via decomposition or charge transfer processes of O_2, O^{2-}, OH^-, and N_2O [18]. It has also been suggested that decomposition of N_2O on metal oxides surfaces such as V_2O_5/SiO_2, MoO_3/SiO_2 and WO_3/SiO_2, leads to the formation of an anion of O^-, which has been claimed to be responsible for the formation of phenol, while O_2 generates O^{2-} on the same metal oxides, and O^{2-} has been reported to cause the scission of carbon to carbon bonds of benzene to give maleic acid or maleic anhydride.

We believe that the N_2O oxidation results with catalyst A and B may be best rationalized by the following mechanistic path, that has been postulated by Iwamoto et al. [18]:

$$N_2O + e^- \text{ (from catalyst)} \longrightarrow O^- + N_2$$

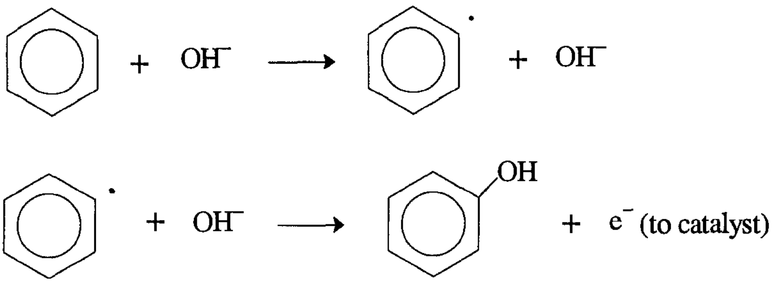

Table 3
Comparison of N_2O oxidation of benzene over catalysts A, B and C

Support matrix	HAMS-1B-3							SiO_2	
Catalyst Prep. method	A CVD			B impregnated				C coformed	
Temp. (°C)	250–350	350	410	335	385	385–425	400	335	335–410
benzene conv. (%)	1	8	17	2	9	9	5	0.2	0.5
product selectivity (%)									
phenol	~ 100	~ 100	97	~ 100	~ 100	~ 100	~ 100	~ 100	~ 100
unidentified		trace	3						
recovery (%)	85	90	84	96	82	93	91	94	88

Catalyst D (borosilicate molecular sieve itself) containing 1.7 wt% B (HAMS-1B-3 prepared in ethylenediamine) was calcined in air at 500°C for 5 h, and loaded into a 1.7" bed in a quartz reactor. The N_2O oxidation of benzene was carried out under the standard running conditions to assess the effect of the molecular sieve itself. The results are summarized along with those obtained in the runs with NO_2 in the presence of steam in table 4.

The borosilicate itself without metal components shows a rather limited catalyt-

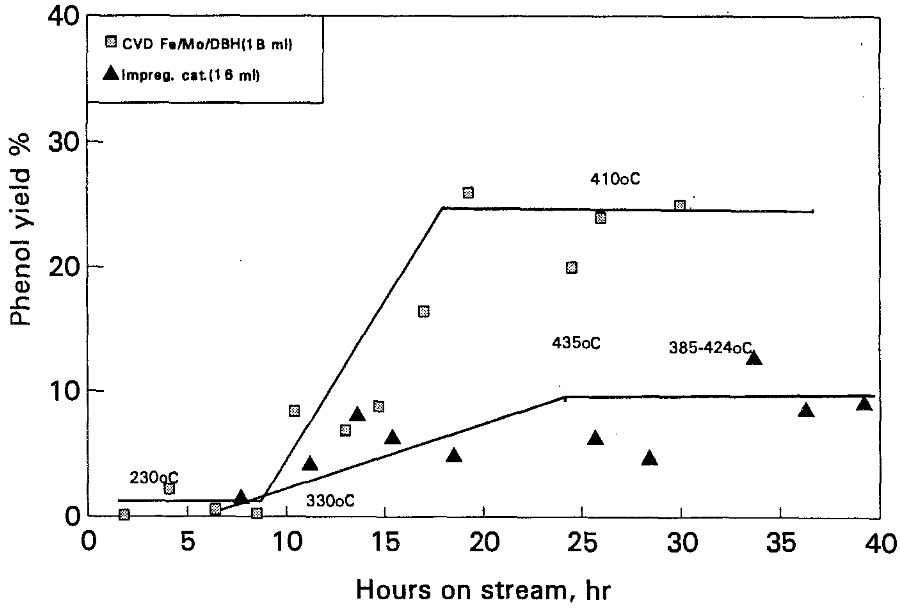

Fig. 4. Synthesis of phenol from benzene by N_2O oxidation. CVD Fe/Mo/DBH versus impregnated Fe/Mo/DBH, LVHSV = 0.1/h, temp. = 230–410°C (CVD), 330–435°C (impregnated).

Table 4
N_2O oxidation of benzene with catalyst D (HAMS-2B-3), N_2O/benzene = 4.4/1, LHSV = 0.1/h

	Temperature (°C)			
	250	300		325
benzene conv. (wt%)	0.5	1.4	(1.7) [a]	2.1
product selectivity (%)				
phenol	~ 100	~ 100	(79)	~ 100
nitrobenzene			(21)	
unidentified	trace	trace	(tr)	trace
phenol recovery (%)	85	93	(97)	87

[a] NO_2 with steam.

ic activity (less than 3%) for the N_2O oxidation of benzene to phenol at 250–325°C, while phenol is produced in low yield. In order to compare this result with that of NO_2 oxidation, the catalyst resulting from the N_2O oxidation was subjected to the NO_2 oxidation in the presence of steam. Phenol was produced in 79% selectivity along with nitrobenzene, a minor product, although the conversion of benzene was limited to only 1.7%. Whereas, nitrobenzene was the only product when benzene was oxidized with NO_2 in the vapor phase over supported benzenesulfonic acid and substituted benzenesulfonic acids [28], HZSM-5 catalyzed the same N_2O oxidation reaction of benzene to phenol [28,29]. Considering the large difference in the acid strength between HZSM-5 and borosilicate (HAMS-1B-3), it is surprising to observe the formation of phenol by the N_2O oxidation with the borosilicate, HAMS-1B-3. Tarry material was formed on the bottom end of the reactor below the heating zone over the HAMS-1B-3 matrix even at 350°C, while catalyst A did not show the same phenomenon until the reaction temperature reached above 425°C. Another batch of borosilicate molecular sieve sample prepared in the caustic medium, HAMS-1B-1, containing sodium, showed no activity for N_2O oxidation.

Judging from these facts, the Brønsted acid sites on borosilicate must be responsible for the phenol formation. The hydroxydiazonium cation is suggested as a plausible reaction intermediate for the hydroxylation of benzene to phenol by an analogy with the mechanism proposed in previous work [29].

Since a strong acid site was seen on the CVD Fe/DBH as shown in fig. 1, it is possible that CVD Fe/DBH may favor the formation of the hydroxydiazonium cation intermediate via interaction of N_2O with the strong acid site, and thus may become a more active system than the borosilicate molecular sieve itself for the phenol formation. The results observed with Fe/H-ZSM-5 [13–15] by Panov et al. may be explained by the same mechanism based on the OH^+ species derived from the hydroxydiazonium cation since it is anticipated to generate stronger acid sites by incorporating iron onto H-ZSM-5, as in the case of Fe/DBH:

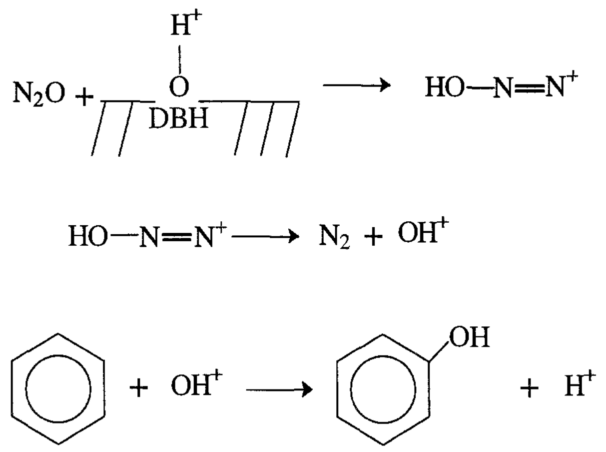

4. Conclusions

The CVD Fe/Mo/DBH catalyst exhibited better catalytic performance for the N_2O oxidation of benzene to phenol than the impregnated counterpart, while the silica coformed catalyst, $Fe/Mo/SiO_2$, was inactive. However, the borosilicate molecular sieve matrix itself was active.

Two mechanistic paths are proposed based on reactive surface oxygen species such as O^-, which can be generated by interaction of N_2O with iron sites in the CVD borosilicate molecular sieve catalyst, or OH^+, which can be generated by the Brønsted acid sites on the molecular sieve itself.

The transmission electron micrographs (TEM) show that fine catalyst particles are uniformly deposited along the main channel of the FMI structure on the CVD catalyst, and that large aggregated particles are deposited in a non-uniform manner mostly on the exterior surface for the impregnated counterpart. Differences in catalytic activity observed between CVD and impregnated catalysts are reflected on the unique structure tailored by the chemical vapor deposition technique.

References

[1] M.S. Kharasch, A. Fono and W. Nudenberg, J. Org. Chem. 15 (1950) 748.
[2] S. Ito, A. Kunai, H. Okada and K. Sasaki, J. Org. Chem. 53 (1988) 296.
[3] A. Kunai, K. Ishihata, S. Ito and K. Sasaki, Chem. Lett. (1988) 1967.
[4] J.S. Yoo, R.A. Sohail and S.S. Grimmer, to be published.
[5] S.S. Shepelov and K.G. Inoe, React. Kinet. Catal. Lett. 23 (1983) 319.
[6] J.R. Anderson and P. Tsai, J. Chem. Soc. Chem. Commun. 19 (1987) 1435.
[7] H.F. Liu, R.S. Liu, K.Y. Liew, R.E. Johnson and J.H. Lunsford, J. Am. Chem. Soc. 106 (1984) 4117.
[8] K. Otsuka and T.J. Nakajima, J. Chem. Soc. Faraday Trans. I 83 (1987) 1315.
[9] H. Yamamoto, H.Y. Chu, M. Xu, C. Shi and J.H. Lunsford, J. Catal. 142 (1993) 325.

[10] R. Burch and C. Howitt, Appl. Catal. A 106 (1993) 167.

[11] R. Burch and C. Howitt, Appl. Catal. A 103 (1993) 135.

[12] R. Burch and C. Howitt, Appl. Catal. A 86 (1992) 139.

[13] V.I. Sobolev, G.I. Panov, A.S. Kharitonov, V.N. Romannikov, A.M. Volodin and K.G. Ione, J. Catal. 139 (1993) 435.

[14] G.I. Panov, V.I. Sobolev and A.S. Kharitonov, J. Mol. Catal. 61 (1990) 85.

[15] G.I. Panov, G.A. Sheveleva, A.S. Kharitonov, V.N. Romannikov and L.A. Vostrikova, Appl. Catal. A 82 (1992) 31.

[16] G.J. Hutchings, M.S. Scurrell and J.R. Woodhouse, J. Chem. Soc. Faraday Trans. I 85 (1989) 2507.

[17] G.J. Hutchings and M.S. Scurrell, in: *Methane Conversion by Oxidative Processes*, ed. E.E. Wolf (Van Nostrand-Reinhold, New York, 1992) p. 200.

[18] M. Iwamoto, J. Hirata, K. Matsukami and S. Kagawa, J. Phys. Chem. 87 (1983) 903; Shokubai 24 (1) (1982) 103; 24 (4) (1982) 276; 26 (6) (1984) 30.

[19] M. Iwamoto, Yuki Gosei Kagaku Kyokaishi 40 (8) (1982) 694.

[20] M. Iwamoto, Shokubai 26 (1) (1984) 30.

[21] M. Iwamoto and J.H. Lunsford, J. Phys. Chem. 84 (1980) 3079.

[22] A.G. Anshits, E.N. Voskresenskaya and L.I. Kurteeva, Catal. Lett. 6 (1990) 67.

[23] C.H. Lin, K.D. Campbell, J.-X. Wang and J.H. Lunsford, J. Catal. 90 (1986) 534.

[24] K. Otsuka and K. Jinno, Inorg. Chem. Acta 121 (1986) 237.

[25] D.J. Drisoll, W. Matin, J.-X. Wang and J.H. Lunsford, J. Am. Chem. Soc. 107 (1985) 58.

[26] V.D. Sokolovskii, S.M. Aliev, O.V. Buyevskaya and A.A. Davydov, Catal. Today 4 (1989) 293.

[27] S.L. Kaliaguine, B.N. Shelimov and V.B. Kazansky, J. Catal. 55 (1978) 384.

[28] Y. Ono, K. Tohmori, S. Suzuki, K. Nakashiro and E. Suzuki, in: *Heterogeneous Catalysis and Fine Chemicals*, ed. M. Guisnet (Elsevier, Amsterdam, 1988) p. 75.

[29] S. Suzuki, K. Nakashiro and Y. Ono, Chem. Lett. (1988) 953.

[30] J.S. Yoo, D.A. Donohue, M.S. Kleefisch, P.S. Lin and S.D. Elfline, Appl. Catal. A 105 (1993) 83.